A simple model for non-topological defects in sheared nematic polymer monodomains

Eric P. Choate
Department of Mathematics, Industrial Mathematics Institute,
University of South Carolina,
Columbia, SC 29208, USA

M. Gregory Forest
Department of Mathematics, Institute for Advanced Materials,
University of North Carolina at Chapel Hill,
Chapel Hill, NC 27599-3250, USA

Lingxing Yao
Department of Mathematics
University of Utah
Salt Lake City, UT 84112, USA

Xiaoyu Zheng
Department of Mathematical Sciences
Kent State University
Kent, OH 44242, USA

Ruhai Zhou
Department of Mathematics and Statistics
Old Dominion University
Norfolk, VA 23529, USA

December 18, 2008

Abstract

Nematic fluids have a propensity for orientational defects. In Leslie-Ericksen theory for small molecule liquid crystals, defects are topological in nature and easily visible in textural snapshots. However, kinetic and mesoscopic theories of nematic polymers possess a richer class of defects, including non-topological defects in which the second moment tensor of the orientational probability distribution fails to uniquely define a major director. These defects include the isotropic phase, where the major director lies anywhere on the unit sphere, and so-called oblate defect phases where the major director lies on a circle in the plane normal to a well-defined minor axis. These isotropic and oblate defect phases are independent of the physical space dimension, and while they have appeared in dynamics of heterogeneous attractors [5, 12, 13], a simple monodomain model of defect phases has not previously been developed. Here we present such a model by restricting to the in-plane monodomain response to an imposed shear flow. The orientational dynamics are described by a three-dimensional dynamical system on a compact domain. We show that the set of isotropic and oblate defect phases separates this compact orientational space into two sets of well-defined orientational distributions, one parallel and another orthogonal to the vorticity axis. We identify orbits that pass through the oblate defect set, and how often they do so. Finally, we observe intriguing behavior at the tumbling-wagging bifurcation where limit cycles pass infinitely often through the oblate defect set.

2000 Mathematics Subject Classification. 76A15, 82D60.
Keywords: Liquid crystal polymers, defects, shear flow

1 Introduction and motivation

Nematic liquid crystals are well known for their display applications and for their beautiful visual patterns under polarized light. These patterns arise from defects in the molecular alignment, that is, locally ordered phases intertwined with locations (points or lines) at which the high aspect ratio molecules do not collectively possess a well-defined preferred direction of orientation. For small molecule liquid crystals, Leslie-Ericksen (LE) theory describes the molecular orientation with a norm-1 vector field $\mathbf{n}$ called the major director that gives the most likely direction of molecular alignment. One success of LE theory is that it admits spatial discontinuities in this orientational vector field, which has proved to be a good model for topological defects. These defects are classified by their winding numbers, often used to define their strength, with values ± 1 or $\pm\frac{1}{2}$ [3].

However, LE theory is unable to regularize these topological singularities, which requires some additional degrees of freedom to resolve defect cores. It is well-known now that the cores of defects either correspond to disordered phases [11, 1, 2] (the maximally disordered isotropic phase, or the partially disordered oblate phase), or the principal axis simply escapes to into the third dimension without any disordered phase at the core [10]. Attempts to couple a scalar order parameter to the LE theory were designed to overcome this limitation [4]. However, the partially disordered oblate phase is not captured by this expanded model nor by complex scalar models, and one is led to at least a tensorial order parameter description [6]. A tensorial order parameter provides sufficient degrees of freedom it is possible to resolve the cores of

defects and remove the apparent singularity of director theory [11]. Kinetic theory uses an orientational probability density function $f(\mathbf{m})$ to describe the likelihood that an individual molecule's axis of symmetry is parallel to the unit vector $\mathbf{m}$, while Landau-deGennes tensor models formulate equations directly for the second-moment tensor

$$\mathbf{M} = \langle \mathbf{mm} \rangle = \int_{\|\mathbf{m}\|=1} \mathbf{mm} f(\mathbf{m})\, d\mathbf{m}, \tag{1}$$

or its traceless counterpart, the orientation tensor $\mathbf{Q} = \mathbf{M} - \frac{\mathbf{I}}{3}$. Whether treated as the primitive variable or post-processed from a kinetic theory calculation of f, $\mathbf{M}$ determines both a local orthonormal frame of directors and also two independent scalar order parameters that provide information about how strongly the molecules are aligned with this frame. These order parameters can describe the nematic phase (where a principal axis of orientation is identified) and the maximally disordered isotropic phase, and the partially disordered oblate phase. These scalar order parameters are local diagnostics of the orientational distribution of the rod ensemble. They can be applied in any space dimensions, including the Onsager phase diagram of equilibria versus rod volume fraction, or space dimension zero; all three nematic, isotropic, and oblate phases play prominent roles in the Onsager phase diagram. These scalar metrics of local orientation also have been applied in three dimensional molecular simulations of M. Allen and collaborators [1] and Callen-Jones [2], as well as in one-dimensional [5] and two-dimensional [12, 13] physical space simulations.

Tensor models possess liquid-crystal-like topological defects associated with director discontinuities, which are regularized through defect cores in two or three spatial dimensions [11, 7, 8, 9], and oblate defects have been found with trivial topology in both one- and two-dimensional heterogeneous shear simulations [5, 12, 13]. Our focus in this paper is a description of these non-topological defects in the simplest possible dynamical situation, a *homogeneous* sample, i.e., "zero space dimensions."

We begin by discussing the orientational information that can be gleaned from the second moment tensor and then identify the tensors that correspond to non-topological defect phases. Then we refine this classification in the presence of a shear flow in the in-plane subspace, and we show that the set of defect phases in orientation space separates logrolling and flow aligning solutions. Finally, we explore the dynamics of a tensor model for sheared monodomains near defect states in two different contexts. First, we examine when a solution may pass through the defect set and change from flow aligning and logrolling or vice versa, and secondly, we discuss the role of oblate defect phases in the tumbling-to-wagging transition.

2 Non-topological defect definitions

The second moment tensor $\mathbf{M}$ is a symmetric, nonnegative definite, rank 2 tensor with trace 1. Therefore, $\mathbf{M}$ defines a quadratic form $\mathbf{m} \cdot \mathbf{M} \cdot \mathbf{m}$, which corresponds geometrically to a triaxial ellipsoid with semiaxes $d_i \mathbf{n}_i$ for the orthonormal frame of eigenvectors $\mathbf{n}_i$ $(i = 1, 2, 3)$ and the corresponding eigenvalues d_i. Note that $0 \leq d_i \leq 1$ and $\sum d_i = 1$. This quadratic form and its ellipsoid can be viewed as a representation of the average molecular orientation in the sense that the direction $\mathbf{m}$ that maximizes $\mathbf{m} \cdot \mathbf{M} \cdot \mathbf{m}$ is the most preferred molecular orientation and the direction that minimizes the quadratic form is the least preferred orientation.

Thus, in order to identify the most preferred direction, we must identify the unique largest eigenvalue of $\mathbf{M}$. Distributions for which $\mathbf{M}$ has a unique largest eigenvalue are called *nematic*. Those without a unique largest eigenvalue define *defect phases* since the principal axis of orientation is no longer specified.

For the nematic phases, eigenvalues of $\mathbf{M}$ satisfy $d_i > d_j \geq d_k$, which also identifies the *major director* $\mathbf{n}_i$ as the eigenvector of $\mathbf{M}$ associated with the unique largest eigenvalue.[1] The remaining two eigenvalues specify a further subdivision into two types of nematc distributions:

If $\mathbf{M}$ has three distinct eigenvalues $d_i > d_j > d_k$, then the corresponding distribution is called *biaxial*. The eigenvector corresponding to the unique middle eigenvalue is called the *minor director* $\mathbf{n}_j$, and it indicates the direction of a secondary bias in the molecular orientation. As a example, suppose that

$$\mathbf{M} = \frac{1}{6}\begin{pmatrix} 3 & 0 & 0 \\ 0 & 2 & 0 \\ 0 & 0 & 1 \end{pmatrix}. \tag{2}$$

On average the molecules are aligned with the major director $\mathbf{e}_x$, but because $\mathbf{e}_y$ is the minor director, the axis of symmetry of a molecule is more likely to lie in the x-y plane than the x-z plane.

If however $\mathbf{M}$ has a repeated second largest eigenvalue $d_i > d_j = d_k$, then the minor director cannot be defined, and the distribution is symmetric with respect to rotation around its major director $\mathbf{n}_i$. Such a distribution is called *uniaxial*, and the ellipsoid defined by $\mathbf{M}$ is a prolate spheroid. For the purposes of this paper, the practical differences between uniaxial and nearby biaxial distributions are insignificant. In either nematic case, there is a clearly defined preferred orientation, the major director $\mathbf{n}_i$.

There are also two distinct types of defect distributions. First, there is the special case in which $\mathbf{M}$ has only one distinct eigenvalue $d_i = d_j = d_k = \frac{1}{3}$. In this case, there is no distinguished direction whatsoever, and so it represents the *isotropic phase*, and its orientation ellipsoid is a sphere. If $d_i = d_j > d_k$, the ellipsoid defined by $\mathbf{M}$ is an oblate spheroid with the maximum orientation occurring anywhere on a circle in the plane orthogonal to $\mathbf{n}_k$. Such a state is therefore called an *oblate defect phase*.

3 Shear-induced defects

We proceed now to a highly studied model for sheared orientational dynamics and impose some geometric controls that highlight defect phases. In the monodomain limit, we assume $\mathbf{M}$ has no spatial gradients, and we can assume a simple shear flow in Cartesian coordinates (x, y, z),

$$\mathbf{v} = De\,(y, 0, 0)^T, \tag{3}$$

where we have used the shear rate $\dot{\gamma}$ and the timescale of molecular relaxation t_r to define the nondimensional Deborah number $De = \dot{\gamma} t_r$. The corresponding rate of strain

[1] Since we have idealized the molecules as non-polar spheroids, $f(\mathbf{m}) = f(-\mathbf{m})$, a symmetry reflected in the quadratic form and its ellipsoid. Thus, the eigenvectors of $\mathbf{M}$ define principal axes, not directors, with $\pm\mathbf{n}_i$ being the major axis. Additionally, we should note that this is the direction that maximizes the second moment tensor ellipsoid, and not necessarily f itself.

and vorticity tensors are

$$\mathbf{D} = \frac{De}{2}\begin{pmatrix} 0 & 1 & 0 \\ 1 & 0 & 0 \\ 0 & 0 & 0 \end{pmatrix}, \ \mathbf{\Omega} = \frac{De}{2}\begin{pmatrix} 0 & 1 & 0 \\ -1 & 0 & 0 \\ 0 & 0 & 0 \end{pmatrix}. \tag{4}$$

This velocity field imposes a symmetry with respect to the flow(x)-flow gradient(y) shearing plane. Specifically, the five-dimensional tensor models for $\mathbf{Q} = \mathbf{M} - \frac{\mathbf{I}}{3}$ possess both a symmetry with respect to this plane and also a three-dimensional subspace. This so-called "in-plane" subspace consists of the tensors $\mathbf{Q}$ in which one eigenvector, labeled $\mathbf{n}_3 = (0, 0, 1)^T$, is always confined to the vorticity direction (z axis), and the two remaining eigenvectors are confined to the x-y plane. We parameterize the one remaining degree of freedom in the eigenvectors as

$$\mathbf{n}_1 = (\cos\psi, \sin\psi, 0)^T, \quad \mathbf{n}_2 = (-\sin\psi, \cos\psi, 0)^T, \tag{5}$$

for the so-called *director angle* ψ. We will restrict to this in-plane subspace for the remainder of this paper.

The restriction $\mathbf{n}_3 = \mathbf{e}_z$ forces $Q_{xz} = Q_{yz} = 0$ so that the orientation tensor takes the form

$$\mathbf{Q} = \begin{pmatrix} Q_{xx} & Q_{xy} & 0 \\ Q_{xy} & Q_{yy} & 0 \\ 0 & 0 & -Q_{xx} - Q_{yy} \end{pmatrix}. \tag{6}$$

The eigenvalues d_i of $\mathbf{M} = \mathbf{Q} + \frac{\mathbf{I}}{3}$ can be written explicitly as

$$\begin{aligned} d_{1,2} &= \tfrac{1}{3} + \tfrac{1}{2}\Big(Q_{xx} + Q_{yy}\Big) \pm \tfrac{1}{2}\sqrt{4Q_{xy}^2 + (Q_{xx} - Q_{yy})^2}, \\ d_3 &= \tfrac{1}{3} - (Q_{xx} + Q_{yy}). \end{aligned} \tag{7}$$

The spectral theorem is commonly used to express $\mathbf{Q}$ in terms of the differences of the eigenvalues, which for this paper we denote by

$$s = d_1 - d_3, \quad R = d_1 - d_2. \tag{8}$$

Using these so-called order parameters, we can write

$$\mathbf{Q} = s\left(\frac{\mathbf{I}}{3} - \mathbf{n}_3\mathbf{n}_3\right) + R\left(\frac{\mathbf{I}}{3} - \mathbf{n}_2\mathbf{n}_2\right) \tag{9}$$

$$= \frac{s}{3}\begin{pmatrix} 1 & 0 & 0 \\ 0 & 1 & 0 \\ 0 & 0 & -2 \end{pmatrix} + \frac{R}{6}\begin{pmatrix} 3\cos 2\psi - 1 & 3\sin 2\psi & 0 \\ 3\sin 2\psi & -3\cos 2\psi - 1 & 0 \\ 0 & 0 & 2 \end{pmatrix}. \tag{10}$$

It should be noted that due to the labeling in (7), $d_1 \geq d_2$, but the relative ordering of d_3 and d_1 or d_2 remains free. This also implies that $R \geq 0$.[2] It is therefore natural to view the spectral variables $\{R, \psi, s\}$ in cylindrical coordinates with ψ from (5).

The restrictions that $0 \leq d_i \leq 1$ and $\sum d_i = 1$ translate into a triangle of allowable values in R-s space, depicted by the shaded triangle in Figure 1. This triangle may be

[2]Since $\mathbf{Q}$ satisfies the symmetry $\mathbf{Q}(s, R, \psi) = \mathbf{Q}(s - R, -R, \psi \pm \frac{\pi}{2})$, all distinct $\mathbf{Q}$ are accounted for with $R \geq 0$. Replacing R with $-R$ is effectively equivalent to swapping the labels of $\mathbf{n}_1$ and $\mathbf{n}_2$.

rotated by around the pole $R = 0$ to establish the compact spectral solution space in the shape of an inverted cone with an inverted cone removed from its base.

The main advantage of this spectral representation $\{R, \psi, s\}$ is that the defect phases and the uniaxial nematic phases are easily identifiable. From (8), the isotropic defect has $s = R = 0$, and it shows us that in the in-plane subspace, oblate defects occur in two distinct forms, $\{R = 0, s > 0\}$ or $\{s = 0, R > 0\}$. Given the representation of $\mathbf{Q}$ in (10), we observe that these two forms are distinguishable by the number of degrees of freedom used to characterize them. Namely, the $s = 0$ oblate defects have two degrees of freedom, R and ψ, whereas the $R = 0$ oblate defects are specified by only the single parameter s.

One drawback of the spectral representation $\{R, \psi, s\}$ is that the Jacobian of the change of variables from $\{Q_{xx}, Q_{yy}, Q_{xy}\}$ is zero when $R = 0$, in which case, ψ cannot be defined as a function of Q_{xx}, Q_{yy}, and Q_{xy}. However, one distinct class of defects takes precisely this form. From (10), tensors in this class have only one degree of freedom and take the form

$$\mathbf{Q}_{\{R=0\}} = s\left(\tfrac{\mathbf{I}}{3} - \mathbf{n}_2\mathbf{n}_2\right) = \tfrac{s}{3}\begin{pmatrix} 1 & 0 & 0 \\ 0 & 1 & 0 \\ 0 & 0 & -2 \end{pmatrix}. \tag{11}$$

Thus, when $0 < s \leq \frac{1}{2}$, the ellipsoid is an oblate spheroid with the vorticity axis $\mathbf{n}_3 = \mathbf{e}_z$ as the minor axis.

When $R > 0$, the angle ψ is defined, but if $s = 0$, the orientation tensor is

$$\mathbf{Q}_{\{s=0\}} = R\left(\tfrac{\mathbf{I}}{3} - \mathbf{n}_2\mathbf{n}_2\right) = \tfrac{R}{6}\begin{pmatrix} 3\cos 2\psi - 1 & 3\sin 2\psi & 0 \\ 3\sin 2\psi & -3\cos 2\psi - 1 & 0 \\ 0 & 0 & 2 \end{pmatrix}. \tag{12}$$

In this case, the oblate spheroid has minor axis $\mathbf{n}_2(\psi)$. Figure 2 depicts cartoons of these two types of oblate defect ellipsoids.

The uniaxial nematic states also come in two distinct forms which are very similar to (11) and (12) except that their spheroids are prolate. If $R = s$, then

$$\mathbf{Q}_{\{s=R\}} = s\left(\mathbf{n}_1\mathbf{n}_1 - \tfrac{\mathbf{I}}{3}\right) = \tfrac{s}{6}\begin{pmatrix} 3\cos 2\psi + 1 & 3\sin 2\psi & 0 \\ 3\sin 2\psi & -3\cos 2\psi + 1 & 0 \\ 0 & 0 & -2 \end{pmatrix}, \tag{13}$$

which indicates alignment parallel to $\mathbf{n}_1$ and a *flow-aligning*[3] uniaxial state. If $R = 0$ and $-1 \leq s < 0$, $\mathbf{Q}_{\{R=0\}}$ from (11) represents a *logrolling* uniaxial state in which the molecules prefer to be parallel to the vorticity axis $\mathbf{e}_z$.

These two types of uniaxial states are similar to nearby biaxial nematic solutions. If $s < 0$ and $R > 0$, then d_3 is the unique largest eigenvalue. Thus, $\mathbf{n}_3 = \mathbf{e}_z$ is the major director of the biaxial nematic distribution, and the solution is logrolling. However, if $s > 0$ and $R > 0$, d_1 is the unique largest eigenvalue so that the major director $\mathbf{n}_1$ is in the shearing plane and we have a flow-aligning biaxial nematic solution. Thus, we see the important role that the set of $s = 0$ defects plays in the dynamics of in-plane momodomain systems: *If a solution in the in-plane subspace were to pass from*

[3] "Flow-aligning" in this context means simply that the major director lies in the flow-flow gradient plane and hence indicates an alignment making an angle of ψ with respect to the flow direction. No distinction between the asymptotic attractors of either the tumbling or flow-aligning states is made at this time.

a flow-aligning state to a logrolling state, or vice versa, the solution must pass through an $s = 0$ defect state along the way. Furthermore, this is entirely a consequence of the symmetries of the in-plane monodomain subspace and is independent of the model used to determine s, R, and ψ.

4 Behavior around defects

We note that the above discussion about the form of $\mathbf{M}$ and its eigenvalues and eigenvectors follows only from the way in which $\mathbf{M}$ represents a distribution of molecules. It does not depend upon the mathematical model used for the dynamics of $\mathbf{M}$. We now turn our attention to the behavior of a simple dynamical system for a nematic monodomain near the set of defects.

The dynamical equation for $\mathbf{M}$ derived from Doi-Hess kinetic theory is

$$\begin{aligned} \tfrac{d\mathbf{M}}{dt} = \;& \boldsymbol{\Omega}\cdot\mathbf{M} - \mathbf{M}\cdot\boldsymbol{\Omega} + a\left(\mathbf{D}\cdot\mathbf{M} + \mathbf{M}\cdot\mathbf{D} - 2\mathbf{D} : \langle\mathbf{mmmm}\rangle\right) \\ & -\mathbf{Q} + N\left(\mathbf{M}\cdot\mathbf{M} - \mathbf{M} : \langle\mathbf{mmmm}\rangle\right), \end{aligned} \tag{14}$$

where N is a nondimensional concentration parameter characterizing the strength of the Maier-Saupe excluded volume potential, $a = \frac{r^2-1}{r^2+1}$ is the molecular shape parameter for the molecular aspect ratio r, and where we have nondimensionalized time in terms of the molecular relaxation time $t_r = (6D_r^0)^{-1}$ for the averaged constant rotary diffusivity D_r^0. We choose the Doi closure $(\bullet) : \langle\mathbf{mmmm}\rangle \approx (\bullet) : \mathbf{MM}$ to approximate the fourth moment and close (14) on $\mathbf{M}$. We can rewrite (14) for in-plane tensors in terms of the spectral representation as

$$\begin{aligned} \tfrac{dR}{dt} = \;& -R\big(1 + \tfrac{N}{3}(R - 1 + 2(R^2 + s^2 - s - sR))\big) \\ & + \tfrac{a\,De}{3}(2 - R + 2s - 3R^2)\sin 2\psi, \end{aligned} \tag{15}$$

$$\tfrac{d\psi}{dt} = -\tfrac{De}{2}\big(1 - \tfrac{a}{3}\tfrac{2s-R+2}{R}\cos 2\psi\big), \tag{16}$$

$$\begin{aligned} \tfrac{ds}{dt} = \;& -s\big(1 + \tfrac{N}{3}(s - 1 + 2(R^2 + s^2 - R - sR))\big) \\ & + \tfrac{a\,De}{3}(1 + R + s - 3sR)\sin 2\psi. \end{aligned} \tag{17}$$

When there is no flow ($De = 0$), the system reproduces the classical Onsager equilibrium phase diagram, Figure 3. The isotropic defect is stable at sufficiently low concentration ($N < 3$), but for higher concentrations ($N > 3$), the isotropic defect is unstable. When $\frac{8}{3} \le N \le 3$, the anisotropic states (stable and unstable) are uniaxial nematic; however, when $N > 3$, there is an unstable $s = 0$ oblate defect phase. All of these solutions are degenerate in that any constant ψ is also a solution.

Now, when $De > 0$, we observe two situations in which the defect set enters directly into the dynamics of the sheared system.

As observed above, for a biaxial logrolling solution to go to a biaxial flow-aligning state it must pass through the defect state, but now, we are able to further qualify this transition. The unit vector in $\{R, \psi, s\}$ space normal to the defect plane $s = 0$ is $(0, 0, 1)^T$, and from (15)-(17):

$$\left(\tfrac{dR}{dt}, \tfrac{d\psi}{dt}, \tfrac{ds}{dt}\right)^T\Big|_{s=0} \cdot (0, 0, 1)^T = \tfrac{a\,De}{3}(1 + R)\sin 2\psi. \tag{18}$$

Thus, if the shape of molecule is determined ($a > 0$ for rods and $a < 0$ for discs), then the sign of the inner product is determined by $\sin 2\psi$. Only when $0 < \psi < \frac{\pi}{2}$ or $-\pi < \psi < -\frac{\pi}{2}$ may a logrolling solution for rods pass through the defect plane to the flow-aligning space. Similarly, a flow-aligning solution may only pass into the logrolling state when $-\frac{\pi}{2} < \psi < 0$ or $\frac{\pi}{2} < \psi < \pi$. Figure 4 shows a solution that begins flow-aligning and then passes through the defect set to become logrolling and then passes through the defect set again as it returns to a flow-aligning state.

A second example of the appearance of the oblate defect states is in the complex tumbling-wagging transition. The longtime behavior depicted in Figure 4 for $De = 2$ is wagging. That is, the solution oscillates with the director angle ψ visiting only a small range of values between $-16°$ and $-12°$. The variation of the order parameters from a uniaxial solution is small as well. However, as De decreases, the size of this wagging orbit in phase space becomes larger. For values of De near 1, the director angle decreases without bound so that the major director tumbles. The order parameters are well into the nematic region and vary only slightly. While the shape of the distribution remains relatively constant in these tumbling and wagging states, the transition between these states is quite complex involving rapid variations in the degree of focusing and defocusing of the distribution, and it indicates the existence of a solution that passes through the $R = 0$ defect set periodically.

Figure 5 shows three different periodic orbits for values of De near the tumbling-wagging transition in a polar representation of R-ψ phase space. The wagging solution ($De = 1.8225$) spends most of its time in the part of its orbit with a relatively large R, but as the director wags, R rapidly decreases so that ellipsoid briefly becomes very close to oblate. When De decreases to 1.8125, R decreases further reaching the pole in our polar coordinates. For $De = 1.8025$, the orbit has passed through and now encircles the pole, but R becomes very small twice during one full tumble of the director.

Figure 6 shows snapshots in time of the resulting ellipsoids from the solutions for these three values of De as they pass near the $R = 0$ defect set. The initial conditions start on the orbit with $\psi = 0$. For $De = 1.8125$ and $De = 1.8225$, the period is approximately 30, but the tumbling orbit is twice as long and therefore has a period of approximately 60. It is interesting to note that while there is a dramatic qualitative difference between the tumbling and wagging behavior of the director angle for $De = 1.8025$ and $De = 1.8225$, the symmetries of the ellipsoids mean that the ellipsoidal representation of these solutions are very similar.

It is important to note the role of the $R = 0$ defect set in Equation (16). In order for R to pass through 0, it must correspond to ψ passing through either $\pm\frac{\pi}{4}$ or $\pm\frac{3\pi}{4}$ so that $\cos 2\psi = 0$, as illustrated in Figure 5.

5 Conclusion

We have established a framework to identify defect states in liquid crystal polymers based purely on the second moment tensor $\mathbf{M}$ of the orientational probability distribution. The eigenvectors of $\mathbf{M}$ provide a convenient local frame of coordinate axes. The associated eigenvalues of $\mathbf{M}$ represent how strongly the molecules align with this frame, and they may be used to identify defect phases that do not possess a unique maximum direction of orientation.

This defect description is independent of the method used to obtain $\mathbf{M}$ and more

importantly, it is a purely local event in that the only things required to detect a defect at the location $(\mathbf{x}_0, t_0)$ are the eigenvalues of $\mathbf{M}(\mathbf{x}_0, t_0)$. Our model is for the dynamics of a spatially homogeneous sample, but the definition readily extends to simulations of one, two, and three spatial dimensions. It also simplifies defect detection both in that it is not necessary to compute winding numbers, and defects with trivial topology are just as easy to detect.

We have also shown that in order for a monodomain system to change from a logrolling (vorticity-aligned) phase to a flow-aligning phase, it must pass through an oblate defect phase. In the present context, the phase change occurs in the time domain, but it is similar to the spatial defect layers observed in [12, 13] where logrolling anchoring conditions were imposed in a shear cell with one-dimensional heterogeneity but where the long-time asymptotic behavior in the interior of the fluid is flow aligning.

Additionally we examined the appearance of oblate defects in the tumbling-wagging transition. The labeling of these two types of solutions come from the behavior of the eigenvector labeled as the major director; however, near this transition it seems that it is the oscillations of the order parameters that have the greater qualitative effect on the behavior of the solution. In both types of behavior near the transition, the solution oscillates between strongly peaked orientations and orientations very close to oblate defects.

Acknowledgments

This research has been supported in part by the Air Force Office of Scientific Research contract FA9550-06-1-0063, National Science Foundation grants DMS- 0807954, 0502266, 0604891, NASA URETI BIMat award No. NCC-1-02037, and Army Research Office grant ARO 47089-MS-SR.

References

[1] D. Andrienko and M. Allen, *Molecular simulation and theory of a liquid crystalline disclination core*, Physical Review E, **61**, 504-510 (2000).

[2] A.C. Callan-Jones, R.A. Pelcovits, V.A. Slavin, S. Zhang, D.H. Laidlaw, and G.B. Loriot, *Simulation and visualization of topological defects in nematic liquid crystals*, Physical Review E, **74**, 061701 (2006).

[3] S. Chandrasekhar and G.S. Ranganath, *The structure and energies of defects in liquid crystals*, Adv. Phys., **35** (1986), 507-596

[4] J.L. Ericksen, *Liquid Crystals with a Variable Degree of Orientation*, Arch. Rational Mech. Anal. **113**, 97-120 (1991).

[5] M.G. Forest, S. Heidenreich, S. Hess, X. Yang, and R. Zhou, *Robustness of pulsating jet-like layers in sheared nano-rod dispersions*, submitted to J. Non-Newtonian Fluid Mech (2008).

[6] P.G. de Gennes and J. Prost, *The Physics of Liquid Crystals*, Oxford University Press, Oxford, UK (1993).

[7] F. Greco and G. Marrucci, *Molecular Structures of the Hedgehog Point Defects in Nematics*, Mol. Cryst. Liq. Cryst. **210** (1992), 129-141.

[8] D.H. Klein, L.G. Leal, C.J. Garcia-Cervera, and H.D. Ceniceros, *Ericksen number and Deborah number cascade predictions of a model for liquid crystalline polymers for simple shear flow*, Phys. Fluids **19** (2007), 023101.

[9] D.H. Klein, L.G. Leal, C.J. Garcia-Cervera, and H.D. Ceniceros, *Three-dimensional shear-driven dynamics of polydomain textures and disclination loops in liquid crystalline polymers*, J. Rheol. **52** (2008), 837-863.

[10] R.B. Meyer, Phil. Mag. **27**, 405 (1973).

[11] N. Schopohl and T.J. Sluckin, *Defect Core Structure in Nematic Liquid Crystals*, Phys. Rev. Lett. **59** (1987), 2582-2584.

[12] X. Yang, M.G. Forest, W.M. Mullins, and Q. Wang, *Dynamic defect morphology and hydrodynamics of sheared nematic polymers in two space dimensions*, submitted to J. Rheol. (2008).

[13] X. Yang, M.G. Forest, Q. Wang, and W.M. Mullins, *Defects in nematic liquids: algebra trumps topology*, submitted to Phys. Rev. Lett. (2008).

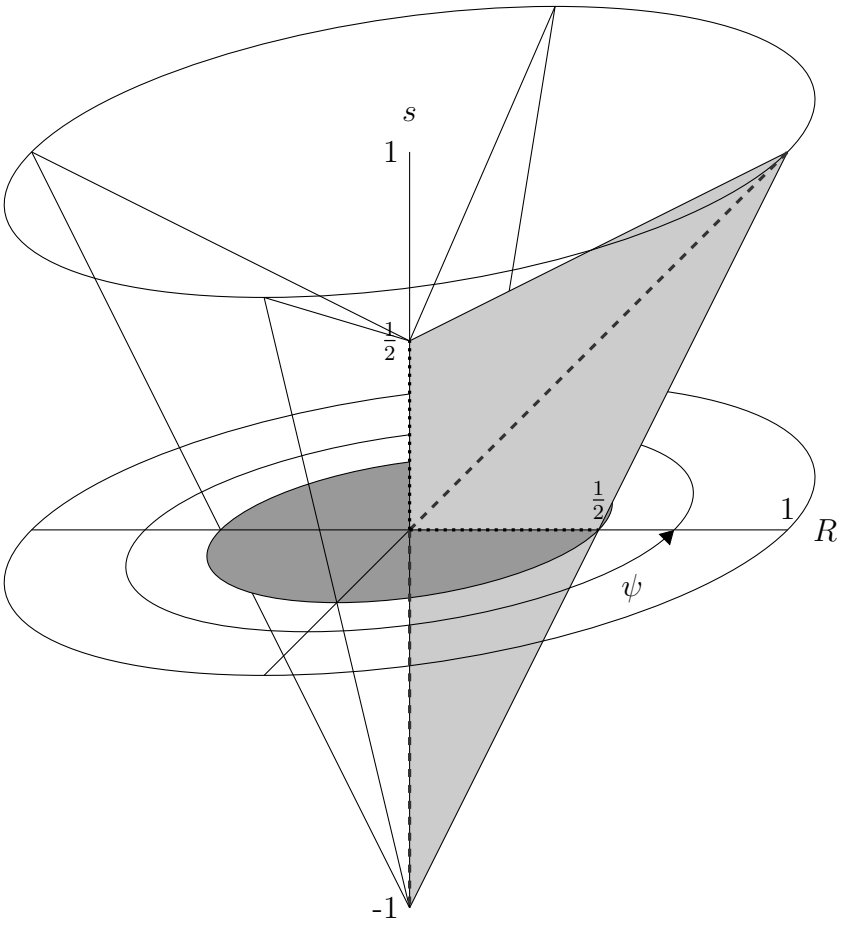

Figure 1: The cylindrical coordinate solution space for in-plane tensors where the order parameters s and R describe are the differences of the eigenvalues and the polar angle ψ parameterizes the eigenvectors of $\mathbf{M}$. The dashed lines correspond to uniaxial states, while the dotted lines (and the disk swept out in rotation) identify the defect set.

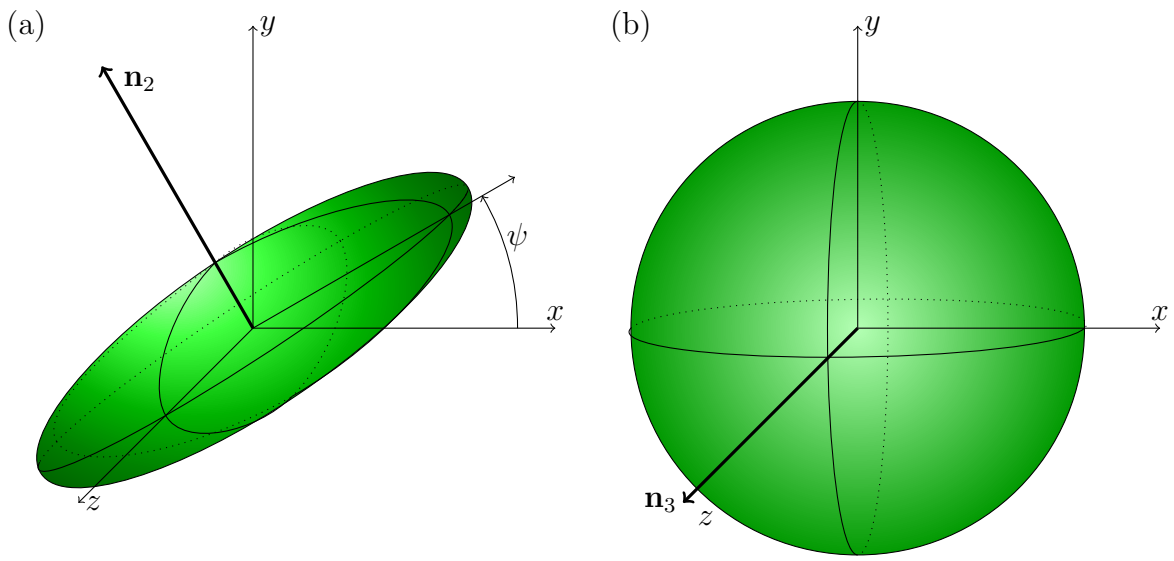

Figure 2: Spheroidal representations of the two different modes of in-plane oblate defects. The ellipsoid in (a) has $s = 0$ and the defect structure is given by $R \approx 0.3$ and $\psi = \frac{\pi}{6}$, but the ellipsoid in (b) has $R = 0$ with $s \approx 0.3$ and no angle ψ can be defined.

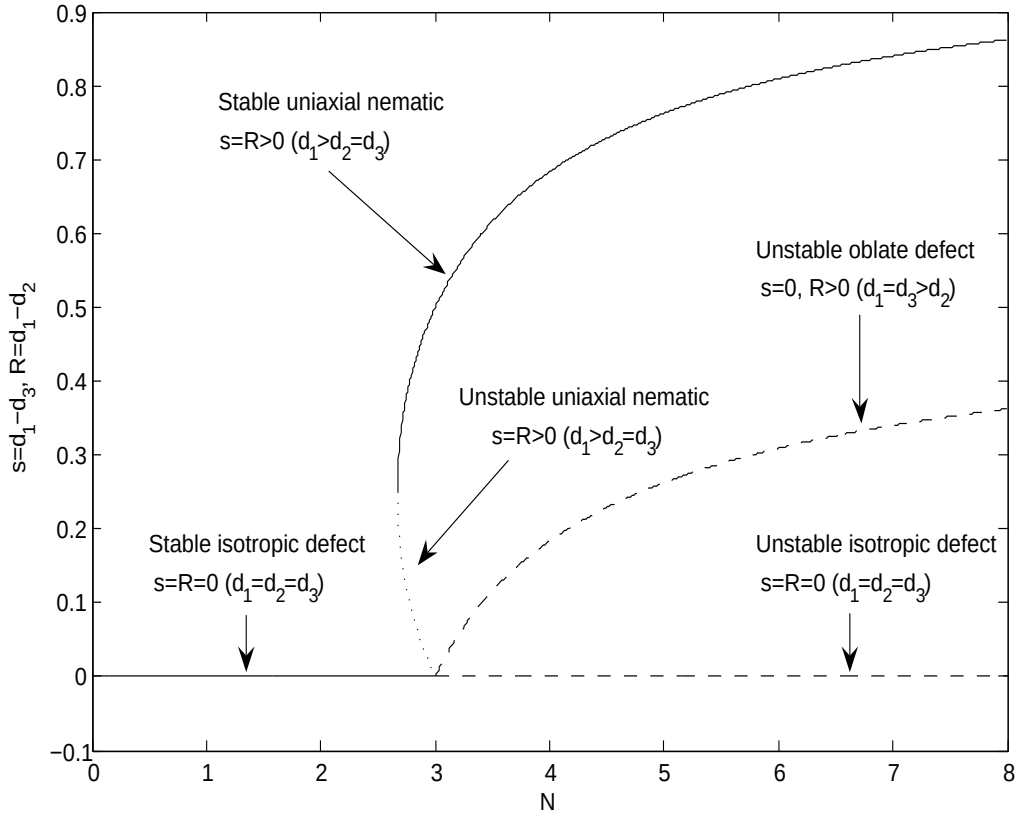

Figure 3: The degenerate steady-state, no-flow equilibrium solutions as a function of the dimensionless concentration parameter N. The solid lines represent stable solutions, either uniaxial nematic or isotropic defect. The dotted line represents an unstable uniaxial nematic solution. The dashed lines represent unstable defect solutions, either isotropic or oblate.

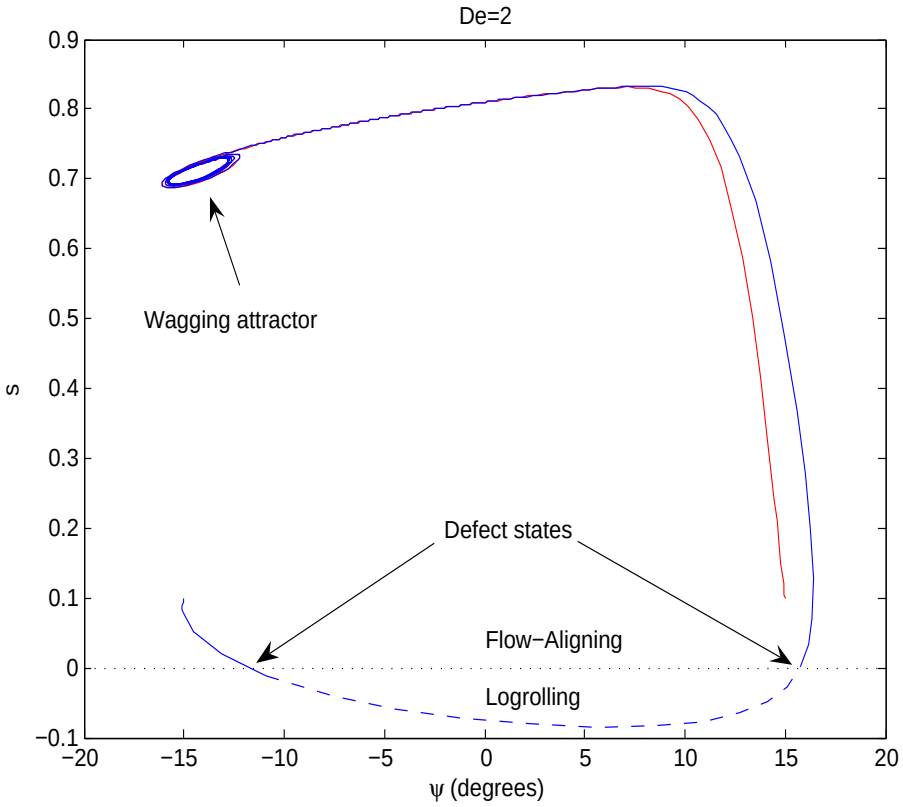

Figure 4: For initial order parameter conditions $s = 0.1$ and $R = 0.45$, and the solutions for both initial angles $\psi = \pm 15^\circ$ begin as flow-aligning (FA) solutions (the solid lines) and approach the same wagging attractor asymptotically. The transient solution for $\psi = 15^\circ$ goes their directly; however for $\psi = -15^\circ$, the solution starts FA and then passes through the $s = 0$ defect set to a logrolling (LR) solution (the dashed line) until ψ becomes positive, at which time it passes back through the defect set as it returns to a FA solution and then approaches the asymptotic solution. ($N = 6$, $a = 0.85$, $De = 2$.)

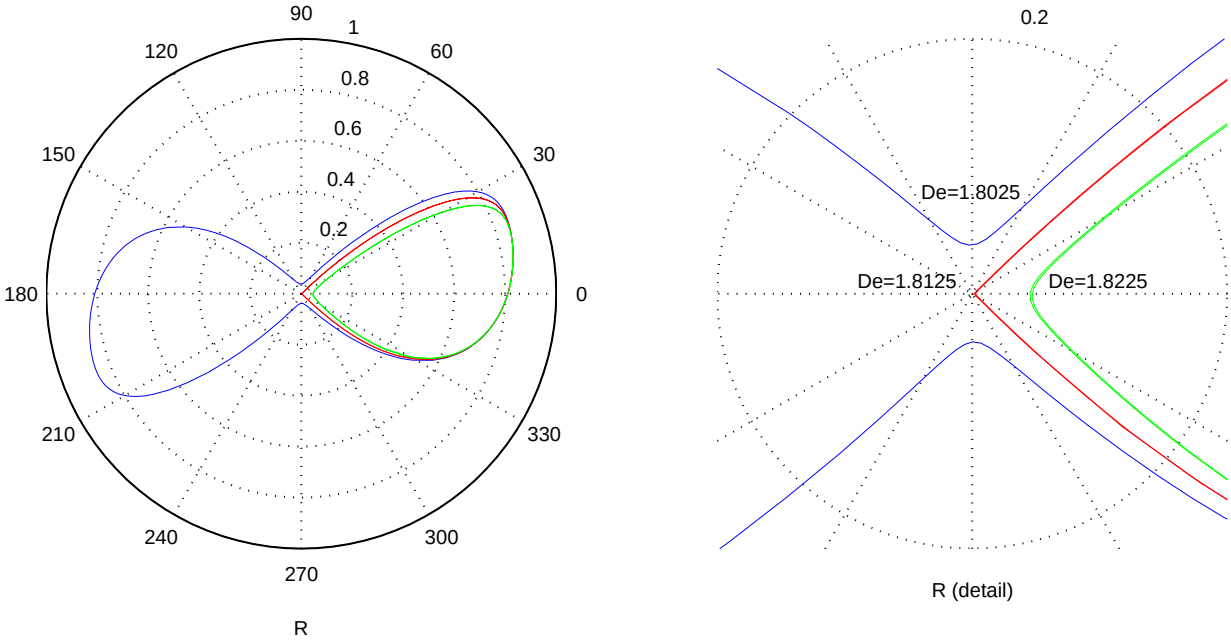

Figure 5: Polar plots of the R-ψ phase space. For $De = 1.8025$, the director tumbles so that ψ visits all angles, but for $De = 1.8225$ the director wags with ψ restricted to a range of approximately 65°. In each of these cases $R > 0$, but in order to transition from one type to the other, it must pass through a transitional orbit in which $R = 0$ periodically.

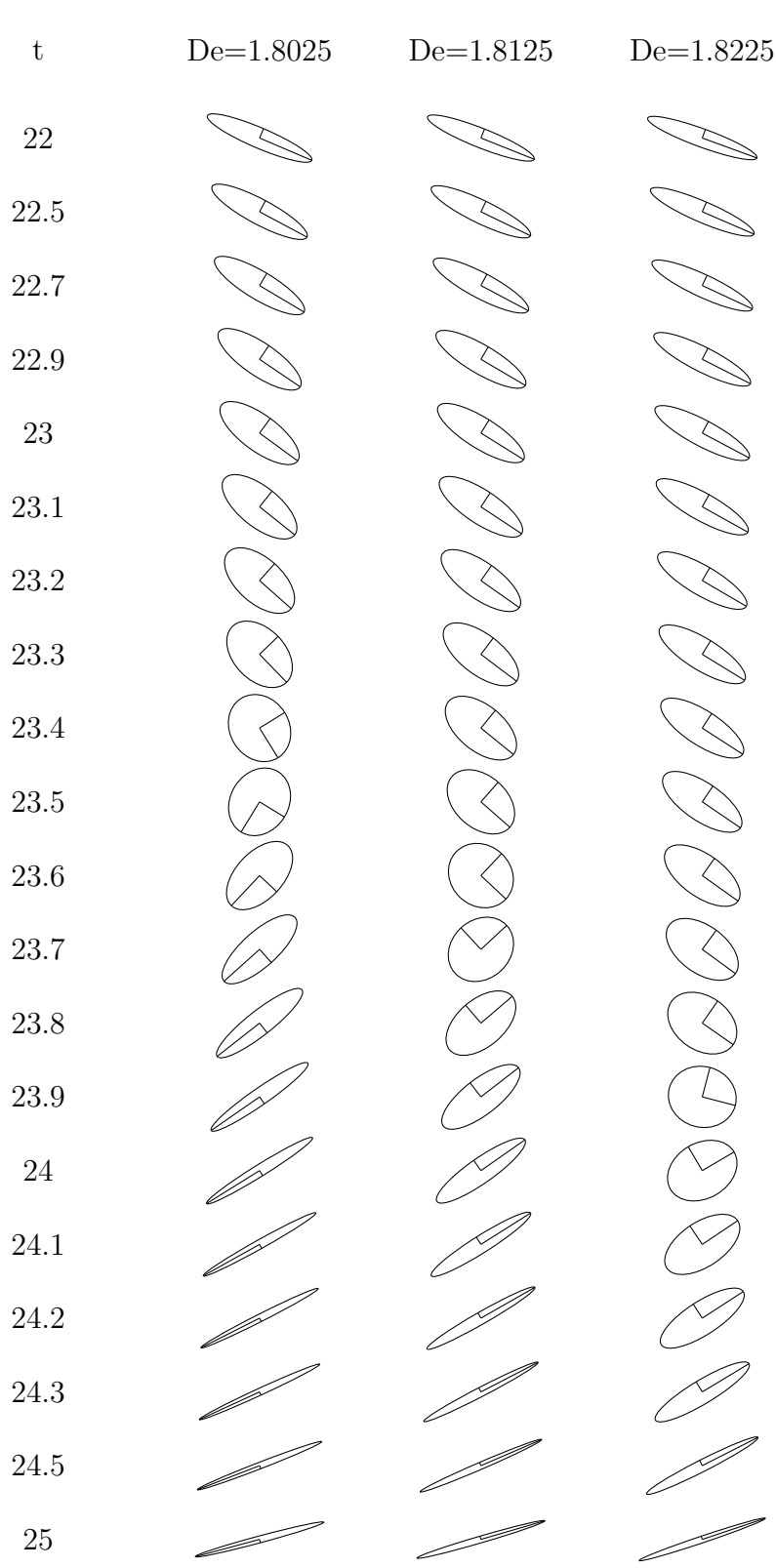

Figure 6: Snapshots in time during the periodic orbits for three values of De near the tumbling-wagging transition. Notice that while the qualitative behavior of ψ is quite different, the resulting shape of the ellipsoids are not.